# Multifunctionality of V-type ATPase during asexual growth and development of *Plasmodium falciparum*

Neeta Shadija[1], Wei Xu[1], Swati Dass[1], Hangjun Ke[1]

[1] Center for Molecular Parasitology, Department of Microbiology and Immunology, Drexel University College of Medicine, Philadelphia, Pennsylvania, USA, 19129

Correspondence, hk84@drexel.edu

## Abstract

V-type ATPases are highly conserved hetero-multi-subunit proton pumping machineries found in all eukaryotic organisms. They use ATP hydrolysis to pump protons, acidifying intracellular or extracellular compartments, and are thus crucial for various biological processes. Despite being evolutionarily conserved in malaria parasites, this proton pump remains understudied. To understand the localization and biological function of V-type ATPase in the deadliest human malaria parasite *Plasmodium falciparum*, we utilized CRISPR/Cas9 to endogenously tag the subunit A of the $V_1$ domain at the C-terminus. $V_1A$ (PF3D7_1311900) was tagged with a triple hemagglutinin (3HA) epitope and TetR-DOZI-aptamers for conditional expression under the regulation of anhydrotetracycline. Through immunofluorescence assays, we identified that V-type ATPase was expressed throughout the intraerythrocytic developmental cycle and was mainly localized on the digestive vacuole and plasma membrane. Immuno-electron microscopy further revealed that V-type ATPase was also localized on secretory organelles, such as rhoptries in merozoites. Knockdown of $V_1A$ led to cytosolic pH imbalance and blockage of hemoglobin digestion in the digestive vacuole, ultimately resulting in parasite growth-arrestment and demise in the trophozoite stage. Using BN-PAGE/Western blot, we detected a large molecular weight complex (~ 1.0 MDa) corresponding to the total molecular weights of $V_1$ and $V_o$ domains. The complex was readily disrupted by the V-type ATPase specific inhibitor Bafilomycin A1, but not by low glucose conditions or treatment with chloroquine. Together, our data suggest that V-type ATPase is localized on several subcellular compartments in *P. falciparum* and plays critical roles to support malaria parasites to grow and replicate inside red blood cells.

## Introduction

Malaria remains one of the deadliest infectious diseases worldwide. In 2021, the WHO reported 247,000,000 malaria cases and 619, 000 deaths[1]. The causative agent of this disease is the protozoan parasite called *Plasmodium*, belonging to the phylum Apicomplexa. Among the five *Plasmodium* species infecting humans (*P. falciparum*, *P. vivax*, *P. ovale*, *P. malariae*, *P. knowlesi*), *P. falciparum* is responsible for the majority of malaria cases and deaths worldwide. All clinical symptoms of malaria arise due to the repetitive growth of the parasites in red blood cells (RBCs); hence, the intraerythrocytic developmental cycle (IDC) or the asexual blood stage has long been recognized as a crucial target for developing antimalarial interventions.

Throughout the IDC, malaria parasites reside in a parasitophorous vacuole and contain many intracellular compartments, including the cytosol, the digestive vacuole (DV) for hemoglobin digestion, the nucleus/ER/Golgi apparatus, the mitochondrion, the apicoplast, and secretory organelles in merozoites. Some of these subcellular compartments are known to have distinct pH, which is key for sustaining the biological processes inside them. For instance, the parasite cytosol maintains a static pH near 7.3[2], whereas the DV requires a lower pH near 5.0 for hemoglobin digestion[3-6]. The mitochondrion has a slightly basic pH (7.37 ± 0.09) whereas the apicoplast is more neutral (7.12 ± 0.40)[7].

Regulation of pH in distinct subcellular compartments involves multiple players, including buffers, enzymes, transporters, and proton pumps[8]. Proton pumps are critical because they can directly transport protons against the concentration gradient, actively regulating pH[9]. In *P. falciparum*, two types of proton pumps are present[10], including the pyrophosphate (PPi) driven $H^+$-pumping pyrophosphatases ($H^+$-PPases) or vacuolar pyrophosphatases (V-PPases)[11-13], and the ATP driven vacuolar type ATPases (V-type ATPases)[14]. VP1 (vacuolar pyrophosphatase 1) is an example of PPi driven proton pumping pyrophosphatase. In *P. falciparum*, a recent study has shown that VP1 is mainly localized on the parasite plasma membrane, regulates cytosolic pH, and plays essential roles in the ring stage and the ring-to-trophozoite transition[15]. On the other hand, V-type ATPase is a large molecular weight ATP hydrolyzing proton pumping machinery[16], consisting of a $V_1$ domain containing subunits of A-H and a $V_o$ domain containing subunits of a, c, c', c'', d, e. $V_1$ holds the ATP hydrolysis hexamer made of A and B subunits, whereas $V_o$ is membrane bound containing the $H^+$ channel, which is involved in proton transport across the membrane. A unique feature of this machinery lies in the reversible assembly and disassembly of the $V_1V_o$ domains[17], regulating the pump's function in response to various extracellular conditions[18]. The *P. falciparum* genome encodes all $V_1$ domain subunits and most $V_o$ domain subunits that are present in other eukaryotes (www.PlasmoDB.org). The recent genome-wide mutagenesis study in *P. falciparum*[19] and the knockout survey in *P. berghei*[20] reveal that nearly all V-type ATPase subunits are essential in the asexual blood stage. Despite its significance, our understanding of the physiological role of V-type ATPase in malaria parasites remains rather limited.

In classical model organisms, including yeast, humans, and plants, V-Type ATPase is localized on the membranes of multiple subcellular compartments such as endosome, lysosomes, vacuoles, Golgi, and the plasma membrane[21-23]. In marine phytoplankton such as diatoms, dinoflagellates and coccolithophores, V-type ATPase localizes to the membranes of chloroplasts derived from endosymbiosis and significantly enhances carbon fixation and oxygen production[24]. In *P. falciparum*, previous studies have suggested that V-type ATPase is a major proton pump responsible for maintaining cytosolic pH[2] and DV pH[5] in trophozoite-stage

parasites. However, its localization has remained elusive or somewhat controversial. An early study indicated that V-type ATPase has heterogenous but not well-defined localization[25]. In another study, immunofluorescence assays (IFAs) and immuno-EM suggested that V-type ATPase is localized on the parasite periphery, DV, and small clear vesicles[26]. However, the use of antibodies raised against the subunits of the bovine V-type ATPase in the study[26] was likely problematic due to limited specificity towards the *Plasmodium* counterparts. Furthermore, another report revealed that V-type ATPase also localizes on the RBC membrane, apparently being exported to the RBC cytosol[27]. Thus, studies of the *Plasmodium falciparum* V-type ATPase have not provided a consensus on its localization. Therefore, further investigation is needed to clarify the localization and function of this important proton pump in malaria parasites.

In this study, we employed genetic and biochemical approaches to better understand the localization and functionality of V-type ATPase in *P. falciparum*. Our data suggest that V-type ATPase is expressed throughout the IDC and exhibits dynamic localization patterns that vary depending on the specific developmental stages of the parasite. We have also discovered the intriguing localization of V-type ATPase on rhoptries and secretory vesicles in merozoites. Moreover, our results underscore the essentiality of V-type ATPase throughout the IDC. Depletion of the proton pump leads to the arrest of trophozoites, which contain undigested hemoglobin in the DV. Using the V-type ATPase specific inhibitor Bafilomycin A1, we have discovered that V-type ATPase potentially plays important roles during parasite egress and invasion. Finally, our study demonstrates that the V-type ATPase is sensitive to disruption by Bafilomycin A1, but the complex stability is less susceptible to certain treatments, such as low glucose or chloroquine.

## Results

### Endogenous tagging of $V_1A$ via CRISPR/Cas9 for localization and conditional knockdown

The highly conserved V-Type ATPase has 2 domains, the $V_1$ domain that hydrolyses ATP and the $V_o$ domain carrying out proton translocation using the free energy released from ATP hydrolysis. *P. falciparum* encodes all subunits required to form the $V_1$ subunit, including subunits of A (PF3D7_1311900), B (PF3D7_0406100), C (PF3D7_0106100), D (PF3D7_1341900), E (PF3D7_0934500), F (PF3D7_1140100), G (PF3D7_1323200), and H (PF3D7_1306600). The $V_o$ includes subunits of a (PF3D7_0806800), c (PF3D7_0519200), c'' (PF3D7_1354400) and e (PF3D7_0721900). Subunits A and B form the ATP hydrolyzing hexamer to power the rotational movement of the entire proton pump. To study V-type ATPase in *P. falciparum*, we successfully tagged the endogenous locus of subunit A ($V_1A$) C-terminally with the triple HA epitope (3xHA) and elements required for conditional knockdown using the TetR-DOZI-aptamer system[28,29]. This was achieved via CRISPR/Cas9[30,31] with two different gRNA plasmids (**Figure 1A**). We termed the resulted transgenic parasite line NF54attB-$V_1A$-3HA$^{apt}$. We also performed limiting dilution to clone the transgenic parasite line to obtain pure parasites. The D11 clone was chosen for all subsequent experiments. The genotype of the NF54attB-$V_1A$-3HA$^{apt}$ line (D11 clone) was verified by diagnostic PCR (**Figure 1B**). The expression of $V_1A$-3HA proteins at the expected molecular weight was confirmed by Western blot (**Figure 1C**).

To verify the localization of V-type ATPase in *P. falciparum*, we tightly synchronized the parasites and performed Immunofluorescence studies (IFAs) over the 48 h lifecycle. We used Exp2[32], the maker for the Parasitophorous Vacuolar Membrane (PVM), as the indicator of the parasite periphery. From the time of invasion (T0), we harvested samples every 8 hours in the ring stage

128 and every 4 hours in trophozoite or schizont stages. $V_1A$ was seen to be expressed in all
129 asexual blood stages (**Figure 2A**). In the ring stage, $V_1A$ localized to the parasite periphery with
130 good colocalization with Exp2. In the trophozoite stage, $V_1A$ was readily observed on the
131 Parasite Plasma Membrane (PPM) and the Digestive Vacuole (DV). This localization pattern
132 was also observed in the early schizont stage. In the late schizont stage, however, some
133 punctate signals appeared near the parasite periphery. To further characterize this, we
134 performed IFA in schizonts that were treated with the egress inhibitor, ML10[33]. ML10 blocks
135 parasite egress by inhibiting pKG, protein kinase G, resulting in an accumulation of mature
136 schizonts that are full of newly formed merozoites. In ML10 treated schizonts, $V_1A$'s localization
137 appeared to be more punctate with no confined signals showing circular or membranous
138 structures (**Figure 2B**). This information prompted us to further verify V-type ATPase's
139 localization in mature schizonts via Immuno-Electron Microscopy. Indeed, immuno-EM revealed
140 a specific localization of $V_1A$ on rhoptries and some small vesicles near them (**Figure 3**),
141 indicating that V-type ATPase is also present on the secretory organelles in merozoites.
142 Altogether, we have used IFA and Immuno-EM to uncover the dynamic localization of V-type
143 ATPase in different asexual stages of *P. falciparum*. This dynamic localization of V-type ATPase
144 may be associated with its multifunctionality throughout the 48 h lifecycle.

145 **V-type ATPase is essential for asexual growth and development in *P. falciparum***

146 To understand the essentiality of V-type ATPase in *P. falciparum*, we performed knockdown
147 studies using two different methods to remove aTc. In the first method, we synchronized the
148 parasites several times and started aTc removal in the early ring stage (**Figure 4A**). The
149 knockdown parasites appeared healthy 24 h post aTc removal, but they failed to produce any
150 new ring stage parasites in the next 24 h. At 48 h of knockdown, the parasites were arrested in
151 the trophozoite stage and became lysed at 72 h. Thus, knockdown $V_1A$ from the early ring stage
152 resulted in trophozoite arrestment and parasite demise within one cycle. In the second method,
153 we started aTc removal from the synchronized trophozoite stage parasites (**Figure 4D**). The
154 knockdown parasites were able to produce new ring stage parasites at 24 h post aTc removal,
155 but they were arrested again in the trophozoite stage at 48 h. The arrested parasites did not
156 initiate another IDC, but remained arrested or lysed at 72 h. Thus, both knockdown methods
157 revealed the essentiality of V-type ATPase for asexual growth and development in *P. falciparum*.
158 In each experiment, quantification of parasite growth in the aTc (±) conditions was shown in
159 **Figure 4B, 4E**. The $V_1A$ protein levels of the knockdown experiments were shown by Western
160 blot in **Figure 4C, 4F**.

161 To better understand parasite developmental blockage upon $V_1A$ knockdown, we observed the
162 morphological changes of the parasites in a more detailed time course experiment (**Figure 4G**).
163 In tightly synchronized parasites, we collected thin blood smears every 8 hours during the ring
164 stage and every 4 hours during the trophozoite and schizont stages. Unlike the aTc (+) parasites
165 that completed their development normally, we observed the arrest of parasite growth in the aTc
166 (-) culture at 32 h post aTc removal. The knockdown parasites were arrested in the mid-
167 trophozoite stage and did not progress significantly in the remaining hours of the IDC.
168 Altogether, using different approaches, we have shown that knockdown of V-type ATPase leads
169 to the arrest of parasite development in the trophozoite stage within one IDC post aTc removal.
170 Overall, our results confirm that V-type ATPase is essential for *P. falciparum*, with the
171 trophozoite stage most susceptible to the loss of this proton pump.

172 **V-type ATPase is essential for hemoglobin digestion**

173 V-type ATPase has been shown to regulate the pH of DV in trophozoite stage parasites[3-5]. To
174 get a deeper understanding of the knockdown effects on the DV, we performed Transmission
175 Electron Microscopy (TEM) studies. The knockdown experiment commenced from Percoll-
176 enriched schizont stage parasites, and we purified parasites by a magnetic column at 36 h post
177 aTc removal. The parasitemia of both aTc (±) cultures reached nearly 100% (**Figure 5A**). The
178 aTc (-) culture displayed more cell lysis compared to the aTc (+) culture after magnetic
179 enrichment, indicating that the integrity of some arrested trophozoites was compromised. Under
180 TEM, the knockdown parasites exhibited striking features (**Figure 5B**). The DV of knockdown
181 parasites showed significantly higher electron density than the control. Additionally, we observed
182 membrane-bound large vesicles inside the DV, indistinguishable from the RBC cytosol in terms
183 of electron density. These structures apparently contained large amounts of undigested
184 hemoglobin. Although not measured quantitatively, we also noticed a significant reduction in
185 hemozoin crystals in the knockdown parasites compared to the control. Consequently,
186 knockdown of V-type ATPase leads to defects in several steps of hemoglobin metabolism,
187 including the release of hemoglobin into the DV, breakdown of hemoglobin into small peptides,
188 and formation of hemozoin.

189 Hemoglobin uptake is initiated at a specialized structure called cytostome[34], and hemoglobin-
190 containing vesicles (HCVs) are pinched off from the membranes and fused with the DV to
191 release their contents for proper digestion and heme detoxification. The hemoglobin containing
192 vesicles are thus wrapped with two membranes, with the PPM on the outside and the PVM on
193 the inside[35]. Interestingly, knockdown of V-type ATPase blocked hemoglobin digestion in the DV,
194 but the upstream trafficking of HCVs en route to the DV was seemingly not affected. This
195 differed from a previous study that showed accumulation of HCVs inside the parasite cytosol
196 upon conditional inactivation of PfVPS45[36], a protein involved in vesicular trafficking. Moreover,
197 the fusion of the outer membrane of HCVs to the DV membrane is potentially a rapid process as
198 this event has been rarely observed in wildtype parasites[37]. In the $V_1A$ knockdown parasites, the
199 undigested hemoglobin was surrounded by a single membrane (**Figure 5B, red arrows**). This
200 information indicated that fusion of HCVs with the DV membrane was likely normal upon
201 depletion of V-type ATPase, but degradation of the inner membrane of HCVs was blocked.
202 Interestingly, we also observed that some vesicles in the DV had much reduced electron
203 density, likely due to a more advanced level of hemoglobin digestion (**Figure 5B, blue arrow**).
204 Overall, our results show that V-type ATPase is critical for hemoglobin release and digestion in
205 the DV.

206 **V-type ATPase is essential for regulating cytosolic pH**

207 Apart from its role in the DV, V-type ATPase is known to regulate cytosolic pH by pumping
208 protons across the PPM in *P. falciparum*[2]. This understanding was based on the observation
209 that Bafilomycin A1, an inhibitor of V-type ATPase, caused a dramatic decline of cytosolic pH. A
210 recent study suggests that Bafilomycin A1 causes a stearic hinderance and blocks the c-ring
211 rotation by preventing the interaction between subunit a and the c-ring[38]. The effect of V-type
212 ATPase on cytosolic pH, however, has not been confirmed by genetic studies in *Plasmodium*. To
213 address this, we utilized the well-established pH measurement technique with BCECF-AM (2',7'-
214 Bis-(2-Carboxyethyl)-5-(and-6)-Carboxyfluorescein, Acetoxymethyl Ester) in saponin-treated
215 trophozoites[2]. We quantified cytosolic pH of aTc ± cultures at 36 h post knockdown from Percoll-
216 enriched schizont stage parasites (**Figure 6**). We included Bafilomycin A1 as a positive control.
217 Our assays revealed that cytosolic pH was 7.24±0.08 in the control parasites but reduced to

218 6.01±0.28 upon knockdown of V-type ATPase. This result confirms that V-type ATPase is the
219 major proton pump for regulating cytosolic pH in trophozoite stage parasites. Consistent with the
220 published data[2], we also observed that Bafilomycin A1 caused a profound decrease in cytosolic
221 pH from 7.24 to 6.51±0.1 within 5 min of treatment. Interestingly, the combination of $V_1A$
222 knockdown and Bafilomycin A1 resulted in an even lower cytosolic pH (5.77±0.15), although this
223 effect was not statistically significant compared to knockdown alone ($p > 0.05$). Overall, our
224 findings confirm that V-type ATPase plays a major role of regulating cytosolic pH in the
225 trophozoite stage.

226 **Viability of the V-type ATPase knockdown parasites**

227 Our experiments have shown that knockdown of V-type ATPase led to the arrest of trophozoite-
228 like parasites that contained large amounts of undigested hemoglobin in the DV and reduced
229 cytosolic pH. To understand the viability of these parasites, we performed an aTc addback
230 experiment post knockdown (**Figure 7A**). In a tightly synchronized culture, we initiated
231 knockdown from Percoll-enriched schizont stage parasites. The addback was carried out at 28
232 h, 36 h, 40 h, and 48 h post knockdown. In consistent with **Figure 4G**, the knockdown parasites
233 at 28 h did not display obvious morphological defects in Giemsa-stained smears (**Figure 7B**).
234 Upon aTc addback, the knockdown parasites were able to produce new ring stage parasites at
235 24 h of addback. At 36 h post knockdown, blockage of parasite development was readily
236 detectable. Upon addback, however, most of the arrested parasites managed to produce new
237 ring stage parasites at 24 h and the ring stage parasites continued to become trophozoites at 48
238 h of addback. This result suggested that the arrested parasites at 36 h post knockdown
239 remained largely viable, despite having severe defects in hemoglobin digestion and pH
240 regulation. At 40 h post knockdown, a smaller percentage of the arrested parasite also
241 succeeded in producing new ring stage parasites at 24 h of addback. However, a few hours
242 later at 48 h post knockdown, aTc addback failed to rescue any parasite growth. The knockdown
243 parasites either displayed abnormal morphologies or lysed. Altogether, these results imply that
244 *P. falciparum* parasites can sustain viability in a severely stressed condition for at least several
245 hours. Apparently, upon aTc addback, restoration of V-type ATPase's activities enables the
246 parasites to digest the accumulated hemoglobin in the DV, raise cytosolic pH to a proper level,
247 and fix other defects due to the loss of this proton pump.

248 **The effect of Bafilomycin A1 on parasite egress and invasion**

249 The localization of V-type ATPase on rhoptries and other secretory organelles prompted us to
250 investigate the potential role of this proton pump in parasite egress and invasion. However, in
251 our knockdown studies initiated from the ring, trophozoite, or schizont stage (**Figures 4-7**), an
252 extended period of ~ 30 h was consistently required before the onset of detectable defects. In
253 addition, all knockdown approaches led to the arrest of trophozoites, making examinations of
254 schizonts infeasible. To address the delayed effects of genetic knockdown, we reasoned that a
255 pool of pre-existing $V_1A$ proteins, present before aTc removal, might permit parasite survival and
256 maturation over an extended period until the proteins were fully exhausted. To overcome this
257 limitation, we used Bafilomycin A1 to rapidly block V-type ATPase in the late schizonts and
258 observed its effect on parasite egress and invasion. As shown previously, Bafilomycin A1
259 reduced cytosolic pH from ~ 7.3 to ~ 6.5 in about 5 min in *in vitro* assays (**Figure 6**).

260 In brief, we tightly synchronized the parasites and used ML10 to block parasite egress, thereby
261 increasing the percentage of mature schizonts. At the mature schizont stage (~ 0 h), we added

262 Bafilomycin A1 (100 nM) for 2 h, washed it out, and allowed parasites to invade new RBCs for 4
263 h. At 6 h post the initiation of the experiment, we counted the parasitemia of newly formed ring
264 stage parasites as the readout of successful egress and invasion (**Figure 8A**). Parasite growth
265 and morphology were also examined at 24 h and 48 h post the initiation of the experiment. At 6
266 h, while the new ring stage reached 4.77%±0.25% in the control culture, the Bafilomycin A1
267 treated culture had a significantly lower parasitemia (0.24%±0.07%) (**Figure 8B**). In the treated
268 culture, events of merozoite invasion were commonly observed, however, formation of new
269 rings was drastically reduced (**Figure 8C**). In the next 24 h and 48 h, the control culture followed
270 the normal progression of the lifecycle. By contrast, the treated culture barely increased parasite
271 numbers (**Figure 8B**). The parasites displayed abnormal morphologies or failed to invade
272 RBCs. We even observed some merozoite-like parasites attaching to the RBC surface at 48 h
273 post the initiation of the experiment (**Figure 8C**). Collectively, treatment of Bafilomycin A1 in the
274 mature schizont stage leads to dramatic reduction in the formation of new ring stage parasites.

275 **Stability of the V-type ATPase complex under various conditions**

276 In model eukaryotes, it has been well established that V-type ATPase undergoes a reversible
277 process of assembly and disassembly to rapidly regulate its function upon encountering
278 different conditions[17]. For example, the yeast V-type ATPase is very sensitive to the bioenergetic
279 status of the cell and $V_1$ and $V_o$ disassociate in a low glucose condition[39]. Disassociation of the
280 two domains completely abolishes the proton pumping function as well as the ATP hydrolysis
281 activity of the $V_1$ domain[40]. To assess if the *Plasmodium falciparum* V-type ATPase can regulate
282 its function by changing complex stability, we treated synchronized trophozoite stage parasites
283 with Bafilomycin A1, chloroquine, and 1 mM glucose and verified complex formation through
284 BN/PAGE. In parallel, the expression level of the $V_1$A monomers was monitored by SDS/PAGE.
285 As shown in **Figure 9**, in the control protein lysate, we detected a high-molecular-weight band
286 near the marker of 1.026 MDa, which approximately corresponded to the total molecular
287 weights of the entire V-type ATPase[21]. In addition, smaller bands near the markers of 720 kDa,
288 240 kDa, and 66 kDa were also detected. The nature of these smaller complexes is uncertain at
289 present. They could be assembly intermediates of the complex or degradation products,
290 although enough protease inhibitor cocktails were included throughout the experiment. Upon
291 Bafilomycin A1 (10 nM) treatment, the top band near 1.026 MDa was detectable after 2 h, but
292 gradually decreased in intensity after 4 h and 8 h. By contrast, the monomer $V_1$A remained more
293 stable throughout the time course. This result indicated that the V-type ATPase dissembled upon
294 Bafilomycin A1 treatment longer than 2 h. Upon treatment with chloroquine (100 nM) or 1 mM
295 glucose, however, the top band near 1.026 MDa remained largely constant even after 8 h. The
296 $V_1$A monomer was stably expressed in chloroquine treated samples and gradually decreased in
297 the low glucose treated samples. Together, these data implied that the V-type ATPase complex
298 was readily disrupted by Bafilomycin A1, but not by treatment of chloroquine or a low glucose
299 condition.

300 **Discussion**

301 In this study, we have characterized the essentiality, localization, and biological function of V-
302 type ATPase in *Plasmodium falciparum*. By tagging the $V_1$ domain's subunit A via
303 CRISPR/Cas9, we generated a conditional knockdown parasite line under aTc regulation and
304 obtained several interesting results.

305 We have found that V-type ATPase is essential for *P. falciparum* during asexual growth and
306 development, with the trophozoite stage being particularly vulnerable to death when this proton
307 pump is depleted (**Figures 4-7**). The localization of *P. falciparum* V-type ATPase is highly
308 dynamic throughout the 48 h asexual lifecycle (**Figures 2-3**). Specifically, in trophozoite stage
309 parasites, V-type ATPase localizes to both the parasite plasma membrane (PPM) and digestive
310 vacuole (DV). This localization pattern is consistent with its role in regulating cytosolic pH[2] and
311 DV pH[5]. Our study also demonstrated a drastic reduction in cytosolic pH in the knockdown
312 parasites during the trophozoite stage (**Figure 6**). Moreover, our data suggests that V-type
313 ATPase is also expressed and localized on the PPM in the ring stage. However, we need to be
314 cautious when defining the precise localization of V-type ATPase in the small ring stage
315 parasites. A recent study implied that V-type ATPase does not play a major role in proton
316 pumping during the ring stage, as the pyrophosphate driven proton pump, PfVP1, is essential
317 for this stage[15]. Conditional depletion of PfVP1 blocks ring stage development and the ring-to-
318 trophozoite transition, which is apparently not rescued by the V-type ATPase. This indicates that
319 V-type ATPase might either not fulfill proton pumping across the PPM in the ring stage or have a
320 negligible role. In the late schizont stage, we have observed punctate signals of $V_1A$ in IFA
321 without defined membranous staining (**Figure 2B**). Immuno-EM further revealed $V_1A$'s
322 localization on rhoptries and secretory organelles near rhoptries (**Figure 3**). To our best
323 knowledge, this is the first report that observed such localization of V-type ATPase on mature
324 secretory organelles in protozoa. A previous study highlighted the function of V-type ATPase in
325 facilitating the maturation of secretory organelles in *Toxoplasma gondii*, an apicomplexan
326 parasite related to *Plasmodium*[41], but the presence of V-type ATPase on mature rhoptries or
327 micronemes was not detected[41]. Thus, the unique localization of V-type ATPase on rhoptries
328 and secretory organelles in *Plasmodium* has led us to investigate the role of this proton pump in
329 parasite egress and invasion. To alleviate the slow effect of genetic knockdown, we used
330 Bafilomycin A1 to chemically inhibit V-type ATPase in a short time (2 h) and observed serious
331 defects of the parasites in initiating the next lifecycle (**Figure 8**). Bafilomycin A1's specificity as a
332 V-type ATPase blocker has been well documented and it has been used as a standard reagent
333 in *P. falciparum* studies[2,5]. We quantified the number of new ring stage parasites post
334 Bafilomycin A1 treatment and used it as a readout to indicate the overall effects on parasite
335 egress and invasion. However, our data did not provide detailed mechanisms underlying the
336 mode of action of Bafilomycin A1 in mature schizont stage parasites. It is possible that
337 Bafilomycin A1 exerts its effects through multiple mechanisms, such as killing the schizonts,
338 blocking egress, and inhibiting invasion. Future investigations will be necessary to characterize
339 these processes in detail. Nevertheless, our data implied that V-type ATPase likely plays a role
340 in parasite egress and invasion.

341 In the trophozoite stage, we have discovered that V-type ATPase is extremely important for
342 hemoglobin digestion in the DV. This finding aligns with the well-established role of V-type
343 ATPase in maintaining DV pH[5]. However, we were still astonished by the observation of
344 undigested hemoglobin in the DV in the knockdown parasites (**Figure 5**). To date, the processes
345 of hemoglobin uptake from cytostomes and the delivery of hemoglobin containing vesicles
346 (HCvs) to the DV remain enigmatic in *P. falciparum*. These processes are likely dynamic,
347 transient, and difficult to capture. A previous study reported the rare fusion of one HCv with the
348 DV membrane among > 600 examined thin sections under transmission electron microscopy[37].
349 Since cytostomes are invaginated from the PPM and PVM, the HCvs are enclosed by the PPM
350 on the outside and the PVM on the inside. The fusion event indicates that the PPM of HCvs

351 fuses with the DV membrane[37]. Therefore, the membrane surrounding the undigested
352 hemoglobin in our data should be the PVM, not the PPM. We can speculate that after HCvs are
353 fused with the DV membrane, the leftover PVM needs to be digested first by specific enzymes
354 (likely lipases) before hemoglobin can be digested by aspartic proteases and cysteine
355 proteases[42]. The enzyme responsible for digesting the PVM of HCvs remains unknown, but it is
356 evidently pH dependent and not among the list of enzymes known to digest hemoglobin[43].

357 Moreover, we have detected the native *P. falciparum* V-type ATPase complex by BN/PAGE. In
358 addition to the large molecular weight band near 1.0 MDa, many smaller bands were also
359 detected (**Figure 9**). Though unknown, we speculate that formation of the *P. falciparum* V-type
360 ATPase complex might be complicated if the bands are intermediate products involved in the
361 dynamic assembly and disassembly processes. In mammalian cells, the V-type ATPase was
362 also examined by BN/PAGE but few intermediate complexes were detected[44]. In addition, we
363 noted that the complex was readily disrupted upon Bafilomycin A1 treatment but remained more
364 stable upon challenges of chloroquine and low glucose. The glucose effect on *P. falciparum* V-
365 type ATPase was not expected since low glucose levels are known to dissociate the complex in
366 yeast[39]. This could reflect the unique features of V-type ATPase in *P. falciparum* in a
367 bioenergetically different environment from that of yeast.

368 In summary, our data have provided insights into the localization and functions of V-type ATPase
369 in *Plasmodium falciparum*, which plays critical roles in regulating pH in various subcellular
370 compartments. As we prepared this manuscript, a very recent report by Alder and colleagues
371 also unveiled the localization and function of V-type ATPase in *Plasmodium falciparum*, using an
372 inducible knockout approach[45]. Their study nicely characterized defects related to knockdown of
373 subunit B of the $V_1$ domain and subunits a and c of the $V_o$ domain. Interestingly, our findings
374 from knockdown of $V_1$A align well with those obtained from inducible knockout of $V_1$B. As
375 subunits A and B work together in the ATP hydrolysis center, genetic knockdown (or knockout)
376 of one subunit mirrors the other. Collectively, we have uncovered the dynamic localization of V-
377 type ATPase in the asexual blood stage of *P. falciparum* and shed light on its significance for
378 parasite growth and development.

379 **Figure Legends**

380 **Figure 1. Endogenous tagging of $V_1$A via CRISPR/Cas9 for conditional expression**

381 **A**, Schematic of modifying the $V_1$A genetic locus via CRISPR/Cas9 mediated double crossover
382 recombination. The primer positions were indicated by black arrows with sequences listed in
383 Table 1.
384
385 **B**, Diagnostic PCR/DNA electrophoresis showing the corrected modification of the $V_1$A genetic
386 locus in the D11 clone of NF54attB-$V_1$A-3HA$^{apt}$. The band sizes of PCR products were 0.8 kb
387 (lane 1), 1.2 kb (lane 4), and 1.9 kb (lane 8). One non-specific band was detected in lane 1
388 (star).
389
390 **C**, Western blot showing the expression of $V_1$A-3HA proteins in the transgenic parasite line,
391 NF54attB-$V_1$A-3HA$^{apt}$.
392
393 **Figure 2. Localization of $V_1$A throughout the asexual blood stages**

394 **A**, Localization of $V_1A$ throughout the lifecycle. In the NF54attB-$V_1A$-3HA$^{apt}$ line, $V_1A$ was
395 detected by anti HA and FITC-labeled secondary antibodies. Exp2 was detected by anti-Exp2[46]
396 and TRITC-labeled secondary antibodies.

397 **B**, Localization of $V_1A$ in mature schizont stage parasites. The synchronized late-trophozoite
398 stage parasites were treated with 25 nM of ML10 for 14 h to reach the mature schizont stage.
399 $V_1A$ was detected by anti HA and FITC-labeled secondary antibodies. DNA was stained with
400 DAPI.

401 In each condition, representative images of at least 25 parasites were shown.

402 **Figure 3. Localization of $V_1A$ on secretory organelles in mature schizont stage parasites**

403 **A-F**, Detection of $V_1A$ signals on rhoptries and secretory organelles near rhoptries in the
404 parasite line NF54attB-$V_1A$-3HA$^{apt}$ by immuno-electron microscopy. Bars, 500 nm.

405 **G-H**, Negative control images with the primary antibody omitted throughout the experiment.
406 Bars, 500 nm.

407 **Figure 4. Essentiality of V-type ATPase in the asexual blood stages**

408 Giemsa-stained images showing parasite morphologies resulted from knocking down of $V_1A$
409 from the ring stage (**A**), or from the trophozoite stage (**D**), in the NF54attB-$V_1A$-3HA$^{apt}$ line.

410 Quantification of parasitemia in the aTc +/- cultures (**B, E**). At each time point, parasitemia was
411 determined from counting 1000 RBCs under a light microscope. Error bars indicated the s.d. of
412 three technical measurements.

413 Western blot showing the expression level of $V_1A$ in the knockdown experiments (**C, F**). The
414 same blot was re-probed with anti-Exp2 to show loading controls.

415 **G**, Giemsa-stained images showing parasite morphological changes over the time course
416 experiment.

417 Experiments of A-F were repeated three times. Panel G was repeated two times.

418 **Figure 5. V-type ATPase is essential for hemoglobin digestion in the digestive vacuole**

419 **A**, Giemsa-stained images of control and $V_1A$ knockdown parasites enriched by a magnetic
420 column.

421 **B**, Electron Transmission Microscopic images of control and $V_1A$ knockdown parasites. In the
422 aTc - parasites, many vesicles inside the digestive vacuole had electron dense signals and were
423 surrounded by membranes (red arrows). Some vesicles had translucent appearance but were
424 still surrounded by membranes (blue arrow).

425 **Figure 6. V-type ATPase regulates cytosolic pH in trophozoite stage parasites**

426 At 36 h post knockdown, aTc +/- cultures of the NF54attB-$V_1A$-3HA$^{apt}$ line were subjected to pH
427 measurement using the BCECF-AM method in the absence of presence of 100 nM Bafilomycin
428 A1 (100 nM) for 5 min. Error bars indicated the s.d. of 3-4 measurements in each condition.
429 Statistical analysis was done by student t-test. This experiment was repeated two times.

430 **Figure 7. Viability of the V-type ATPase knockdown parasites**

**A**, Schematic diagram of the knockdown/addback experiment. At various time points post knockdown, the cultures were fed with aTc + medium and further monitored for 48 h.

**B**, Giemsa-stained images showing morphological changes of the parasites upon aTc addback.

This experiment was repeated three times.

**Figure 8. Effects of Bafilomycin A1 on parasite egress and invasion**

**A**, Schematic illustration of the experimental design generated by BioRender. Mature schizont stage parasites (NF54attB-$V_1$A-3HA$^{apt}$ under 250 nM) were treated with Bafilomycin A1 (100 nM) for 2 h. The drug was washed out and parasites were allowed to invade new RBCs for 4 h. At 6 h, the parasitemia of newly formed ring stage parasites was monitored. Parasite morphology and number were further examined at 24 h and 4 h post the initiation of the experiment. aTc (250nM) was maintained throughout the experiment.

**B**, Giemsa-stained imaging showing parasite morphologies in the control and treated cultures.

**C**, Quantification of parasite growth throughout the experiment. Parasitemia was determined by counting 1000 RBCs in each smear under a light microscope. Error bars indicated the s.d. of 3 measurements at each time point.

This experiment was repeated five times.

**Figure 9. The stability of V-type ATPase complex under various conditions**

Synchronized trophozoite stage parasites (NF54attB-$V_1$A-3HA$^{apt}$ under 250 nM) were treated with Bafilomycin A1 (10 nM), Chloroquine (100 nM), or 1 mM glucose for 2 h, 4 h, and 8 h. Samples were harvested and analyzed by BN-PAGE and SDS-PAGE. The arrow indicated the large molecular weight band corresponding to the estimated size of the *P. falciparum* V-type ATPase. aTc (250nM) was maintained throughout the experiment.

465 **Materials and Methods**

466 **Table 1. Primers and oligoes used in this study**

| ID | PRIMER NAME | SEQUENCE |
|---|---|---|
| P1 | A-VATPase gRNA1 | TCATATTAAGTATATAATATTAGTAGGTTTAAGAAACTTGAGTTTCAGAGCTATGCTGGA |
| P2 | A-VATPase gRNA2 | CATATTAAGTATATAATATTGAAACTTGATGGAAAAATGATGTTTCAGAGCTATGCTGGA |
| P3 | A-VATPase gRNA1-N20 | AGTAGGTTTAAGAAACTTGA |
| P4 | A-VATPase gRNA2-N21 | GAAACTTGATGGAAAAATGAT |
| P5 | N20CheckR | ATATGAATTACAAATATTGCATAAAGA |
| P6 | RevOligo | TAGGAAATAATAAAAAAGCACCGACTCG |
| P7 | Super CPF1 | CTTTTATTTTTACTGTAATATAATTTTTTATAATGTAAAAATAAAGGG |
| P8 | A-VATPase 5HRF | gatatctacgatatcccgcggtccggaGGTTCTCCATCTCGTATAGG |
| P9 | A-VATPase 5HRR | ATGGTAACCTGcTTcTCCATaAgaTTaCgaAgtCCaACaGTTATTTCTTCTTCAAGTGCC |
| P10 | A-VATPase 3UTRF | atgcgcgcGTGATTTATTTATTAGTTGAATAATTAAAGC |
| P11 | A-VATPase 3UTRR | tccggaccgcgggatatcgtagatatcGAAAAAGTTTACCTTAGTATGATAAAAAAATG |
| P12 | pMG75-BBHA REV | TGGGCCCGAATTCTCATCATTGTGC |
| P13 | pMG75SeqF | CTTTAAATTCATGCAAAAATTTAC |
| P14 | A-VATPase 5chk | GGTTATCCAGCTTATTTAGGTGC |
| P15 | A-VATPase 3chk New | GATCTACTTACAATTTTTTTCCTTC |

467

468

469 1, Plasmid Construction

470 Subunit A of *Plasmodium falciparum* V-Type ATPase ($V_1A$, PF3D7_1311900) was endogenously
471 tagged with a 3xHA epitope and the TetR-DOZI-Aptamer system at the C-terminus via
472 CRISPR/Cas9. Two NFCas9/gRNA constructs were made according to our cloning procedures
473 published earlier[47]. The DNA oligoes used for cloning and sequencing were listed in **Table 1**
474 (P1-P7). To make the pMG75 template plasmid for double crossover recombination, the 5' and
475 3' homologous regions (5'HR and 3'HR) of $V_1A$ were PCR amplified from the wildtype genomic
476 DNA using primers P8 and P9 for 5'HR and P10 and P11 for 3'HR. The PCR product was
477 purified and then digested with SacII/BstEII for 5'HR and BssHII/SacII for 3'HR. The digested
478 fragments were sequentially cloned into the pMG75 vector bearing Blasticidin deaminase by T4
479 DNA ligase. The clones were screened by proper restriction digestion. The positive clones were
480 further confirmed by Sanger sequencing using the primers P12-P13. The final maxi-prep

481 plasmid of pMG75-BSD-$V_1$A-3HA was linearized with EcoRV before being transfected into
482 parasites.

483 2, Parasite Culture and Transfection

484 *Plasmodium falciparum* wildtype strain NF54attB was generously provided by Dr. Joshua Beck
485 (Iowa State University). This line is compatible with all three transfection markers that are
486 commonly used, including BSD (Blasticidin deaminase), hDHFR (human dihydrofolate
487 reductase) and yDHODH (yeast dihydroorotate dehydrogenase). *P. falciparum* was cultured in
488 human $O^+$ red blood cells (5% hematocrit, Interstate Blood Bank, Inc.) in the standard RPMI
489 1640 medium containing 0.5% AlbuMAX® II (Invitrogen), 15 mM HEPES, 10 mg/L
490 hypoxanthine, 25 mM $NaHCO_3$, and 50 mg/L gentamicin. Transfections were performed using
491 the standard methods in the ring stage with details shown previously[47,48]. The concentration of
492 aTc was 250 nM in all aTc (+) cultures.

493 3, Immunofluorescence assays (IFA)

494 Parasites were tightly synchronized with alanine (0.5 M)/HEPES (10 mM) several times. At each
495 time point of the experiment, ~ 50 µL parasitized RBCs were collected and fixed with 4%
496 paraformaldehyde, 0.0075% glutaraldehyde in 1X PBS. Blocking was done by 3% BSA/PBS for
497 overnight at 4°C. Fixed cells were permeabilized by Triton X-100 (0.25%)/PBS and incubated
498 with primary antibodies overnight at 4°C, including α-HA (1:300, mouse, sc-7392, Santa Cruz
499 Biotechnology) and α-Exp2 (1:500, rabbit)[46]. Following thorough washing, the samples were
500 incubated with FITC- or TRITC- labeled secondary antibodies for 3 h at room temperature.
501 Other procedures followed standard IFA protocols. Images were captured using the Nikon Ti
502 microscope.

503 4, Western Blot for BN-PAGE and SDS-PAGE

504 Parasite cultures were lysed by Saponin (0.05%)/PBS and host hemoglobin was removed by
505 several washes with 1X PBS. From one culture condition, two aliquots of samples were
506 obtained for BN-PAGE and SDS-PAGE, respectively. For BN-PAGE, the saponin lysed pellet
507 was solubilized with 1% glycodiosgenin (GDN) in MESH buffer (250 mM sucrose, 10 mM
508 HEPES, 1 mM EDTA, 1X protease inhibitor cocktail) for overnight at 4°C. The supernatant after
509 a high-speed centrifugation (13,000 rpm, 10 min) was used for Blue-Native gel electrophoresis
510 and Western blot. For SDS-PAGE, the saponin lysed pellet was solubilized by 2% SDS/Tris (65
511 mM, pH 6.8) for overnight at 4°C. The supernatant after a high-speed centrifugation (13,000
512 rpm, 10 min) was used for denatured electrophoresis. For all samples, the protein
513 concentrations were determined by the Pierce™ BCA Protein Assay Kit (ThermoFisher
514 Scientific) to ensure equal loading. Antibodies used for Western blot included α-HA (1:10,000,
515 mouse, sc-7392, Santa Cruz Biotechnology), α-Exp2 (1:10,000, rabbit)[46], HRP-conjugated goat
516 anti-mouse secondary (1:10,000, A16078, ThermoFisher Scientific), HRP-conjugated goat anti-
517 rabbit secondary (1:10,000, 31460, ThermoFisher Scientific). The membranes were incubated
518 with Pierce ECL Western Blot Substrates and developed using the Bio-Rad chemidoc imaging
519 system.

520 5, Transmission Electron Microscopy

521 Parasites were synchronized with alanine (0.5 M)/HEPES (10 mM) several times and the
522 schizont stage parasites were enriched by Percoll. After several washes with 1X PBS, the

523 schizonts were added with new RBCs and cultured in aTc +/- conditions for 36 h. Both cultures
524 were then passed through a MACS magnetic column (MiltenyiBiotec) to enrich trophozoite
525 stage parasites, which were fixed with freshly made 2% paraformaldehyde, 2.5% glutaraldehyde
526 in 100mM sodium cacodylate buffer for overnight at 4°C. The samples were shipped to Dr.
527 Wandy Beatty from the Molecular Microbiology Imaging Facility at Washington University, St.
528 Louis, MO for further processing and imaging. Other procedures were carried out as shown
529 previously[48].

530 6, Immuno-Electron Microscopy

531 Parasites were synchronized with alanine (0.5 M)/HEPES (10 mM) several times and the
532 trophozoite stage parasites were enriched using a MACS magnetic column (MiltenyiBiotec). The
533 enriched parasites were treated with 25 nM ML10[33] for 14 h and then fixed with freshly made
534 4% paraformaldehyde/0.05% glutaraldehyde/100mM PIPES buffer for overnight at 4°C. The
535 samples were shipped to Dr. Wandy Beatty from the Molecular Microbiology Imaging Facility at
536 Washington University, St. Louis, MO for further processing and imaging. Other procedures
537 were carried out as previously published[47]. Antibodies used in the study included α-HA (1:300,
538 mouse, sc-7392, Santa Cruz Biotechnology) and goat anti-mouse IgG 18 nm colloidal gold-
539 conjugated secondary antibody (1:100, Jackson ImmunoResearch Laboratories). A parallel
540 sample with the primary antibody omitted was used as the negative control, which did not react
541 to the secondary antibody.

542 7, pH measurement with BCECF-AM, a ratio-metric pH indicator

543 pH measurement was carried out according to the published protocols[2]. Post 36 h of aTc
544 removal, the control and knockdown cultures were incubated with 4 μM BCECF-AM (2',7'-Bis-
545 (2-Carboxyethyl)-5-(and-6)-Carboxyfluorescein, Acetoxymethyl Ester, Fisher Scientific) for 30
546 min at 37°C. Pluronic at 1:1000 dilution was added to increase cellular permeability to BCECF-
547 AM. The parasites were treated with rapid saponin lysis to remove hemoglobin. The pellet was
548 washed two times with saline/glucose buffer (NaCl 125 mM, KCl 5 mM, MgCl2 1 mM, glucose
549 20 mM, HEPES 25 mM, pH 7.4) and resuspended in 1 mL of warm saline/glucose buffer. The
550 sample's fluorescence was monitored using a fluorescence spectrometer (Hitachi F-7000) at
551 535 nm with excitation wavelengths set at 490/440 nm. When Bafilomycin A1 (100 nM) was
552 used in aTc +/- conditions, the drug was incubated with saponin-lysed and washed parasites for
553 5 min before they were further analyzed by Hitachi F-7000. The fluorescence ratios were back
554 calculated to pH values according to a linear regression curve generated from several known
555 pH standards (pH 6.8, 7.1, 7.4), as shown previously[2].

556 **Acknowledgement**

557 We are grateful for the technical assistance and intellectual input from members of the Center
558 for Parasitology at Drexel University College of Medicine. We thank Dr. Joshua Beck (Iowa
559 State University) for providing the parasite line, Drs. Jaquin Niles (MIT) and Sean Prigge (Johns
560 Hopkins University) for providing the TetR-DOZI-aptamer plasmids, Drs. Baker and Ooij for
561 providing the compound, ML10. We thank Dr. Wandy Beatty at Washington University in St.
562 Louis for performing transmission electron microscopy and immuno-electron microscopy
563 studies.

564

565 **References**


566 1 WHO. World Malaria Report. (2022).
567 2 Saliba, K. J. & Kirk, K. pH regulation in the intracellular malaria parasite, Plasmodium
568 falciparum. H(+) extrusion via a V-type H(+)-ATPase. *J Biol Chem* **274**, 33213-33219
569 (1999). https://doi.org:10.1074/jbc.274.47.33213
570 3 Kuhn, Y., Rohrbach, P. & Lanzer, M. Quantitative pH measurements in Plasmodium
571 falciparum-infected erythrocytes using pHluorin. *Cell Microbiol* **9**, 1004-1013 (2007).
572 https://doi.org:10.1111/j.1462-5822.2006.00847.x
573 4 Bennett, T. N. *et al.* Drug resistance-associated pfCRT mutations confer decreased
574 Plasmodium falciparum digestive vacuolar pH. *Mol Biochem Parasitol* **133**, 99-114
575 (2004). https://doi.org:10.1016/j.molbiopara.2003.09.008
576 5 Saliba, K. J. *et al.* Acidification of the malaria parasite's digestive vacuole by a H+-
577 ATPase and a H+-pyrophosphatase. *J Biol Chem* **278**, 5605-5612 (2003).
578 https://doi.org:10.1074/jbc.M208648200
579 6 Klonis, N. *et al.* Evaluation of pH during cytostomal endocytosis and vacuolar catabolism
580 of haemoglobin in Plasmodium falciparum. *Biochem J* **407**, 343-354 (2007).
581 https://doi.org:10.1042/BJ20070934
582 7 Mohring, F. *et al.* Determination of glutathione redox potential and pH value in
583 subcellular compartments of malaria parasites. *Free Radic Biol Med* **104**, 104-117
584 (2017). https://doi.org:10.1016/j.freeradbiomed.2017.01.001
585 8 Casey, J. R., Grinstein, S. & Orlowski, J. Sensors and regulators of intracellular pH. *Nat*
586 *Rev Mol Cell Biol* **11**, 50-61 (2010). https://doi.org:10.1038/nrm2820
587 9 Cosse, M. & Seidel, T. Plant Proton Pumps and Cytosolic pH-Homeostasis. *Front Plant*
588 *Sci* **12**, 672873 (2021). https://doi.org:10.3389/fpls.2021.672873
589 10 Ginsburg, H. Abundant proton pumping in Plasmodium falciparum, but why? *Trends*
590 *Parasitol* **18**, 483-486 (2002). https://doi.org:10.1016/s1471-4922(02)02350-4
591 11 McIntosh, M. T. & Vaidya, A. B. Vacuolar type H+ pumping pyrophosphatases of parasitic
592 protozoa. *Int J Parasitol* **32**, 1-14 (2002). https://doi.org:10.1016/s0020-7519(01)00325-3
593 12 McIntosh, M. T., Drozdowicz, Y. M., Laroiya, K., Rea, P. A. & Vaidya, A. B. Two classes of
594 plant-like vacuolar-type H(+)-pyrophosphatases in malaria parasites. *Mol Biochem*
595 *Parasitol* **114**, 183-195 (2001). https://doi.org:10.1016/s0166-6851(01)00251-1
596 13 Luo, S., Marchesini, N., Moreno, S. N. & Docampo, R. A plant-like vacuolar H(+)-
597 pyrophosphatase in Plasmodium falciparum. *FEBS Lett* **460**, 217-220 (1999).
598 https://doi.org:10.1016/s0014-5793(99)01353-8
599 14 Karcz, S. R., Herrmann, V. R. & Cowman, A. F. Cloning and characterization of a
600 vacuolar ATPase A subunit homologue from Plasmodium falciparum. *Mol Biochem*
601 *Parasitol* **58**, 333-344 (1993). https://doi.org:10.1016/0166-6851(93)90056-4
602 15 Omobukola Solebo, L. L., Jing Zhou, Tian-min Fu, Hangjun Ke. Malaria parasites utilize
603 pyrophosphate to fuel an essential proton pump in the ring stage and the transition to
604 trophozoite stage. *BioRxiv* (2021). https://doi.org:doi:
605 https://doi.org/10.1101/2021.10.25.465524
606 16 Vasanthakumar, T. & Rubinstein, J. L. Structure and Roles of V-type ATPases. *Trends*
607 *Biochem Sci* **45**, 295-307 (2020). https://doi.org:10.1016/j.tibs.2019.12.007
608 17 Kane, P. M. Disassembly and reassembly of the yeast vacuolar H(+)-ATPase in vivo. *J*
609 *Biol Chem* **270**, 17025-17032 (1995).
610 18 Wang, H. & Rubinstein, J. L. CryoEM of V-ATPases: Assembly, disassembly, and
611 inhibition. *Curr Opin Struct Biol* **80**, 102592 (2023).
612 https://doi.org:10.1016/j.sbi.2023.102592

613 19 Zhang, M. *et al.* Uncovering the essential genes of the human malaria parasite
614 Plasmodium falciparum by saturation mutagenesis. *Science* **360** (2018).
615 https://doi.org:10.1126/science.aap7847
616 20 Bushell, E. *et al.* Functional Profiling of a Plasmodium Genome Reveals an Abundance
617 of Essential Genes. *Cell* **170**, 260-272 e268 (2017).
618 https://doi.org:10.1016/j.cell.2017.06.030
619 21 Harrison, M. A. & Muench, S. P. The Vacuolar ATPase - A Nano-scale Motor That Drives
620 Cell Biology. *Subcell Biochem* **87**, 409-459 (2018). https://doi.org:10.1007/978-981-10-
621 7757-9_14
622 22 Graham, L. A., Flannery, A. R. & Stevens, T. H. Structure and assembly of the yeast V-
623 ATPase. *J Bioenerg Biomembr* **35**, 301-312 (2003).
624 https://doi.org:10.1023/a:1025772730586
625 23 Lupanga, U. *et al.* The Arabidopsis V-ATPase is localized to the TGN/EE via a seed
626 plant-specific motif. *Elife* **9** (2020). https://doi.org:10.7554/eLife.60568
627 24 Yee, D. P. *et al.* The V-type ATPase enhances photosynthesis in marine phytoplankton
628 and further links phagocytosis to symbiogenesis. *Curr Biol* **33**, 2541-2547 e2545 (2023).
629 https://doi.org:10.1016/j.cub.2023.05.020
630 25 Karcz, S. R., Herrmann, V. R., Trottein, F. & Cowman, A. F. Cloning and characterization
631 of the vacuolar ATPase B subunit from Plasmodium falciparum. *Mol Biochem Parasitol*
632 **65**, 123-133 (1994). https://doi.org:10.1016/0166-6851(94)90121-x
633 26 Hayashi, M. *et al.* Vacuolar H(+)-ATPase localized in plasma membranes of malaria
634 parasite cells, Plasmodium falciparum, is involved in regional acidification of parasitized
635 erythrocytes. *J Biol Chem* **275**, 34353-34358 (2000).
636 https://doi.org:10.1074/jbc.M003323200
637 27 Marchesini, N., Vieira, M., Luo, S., Moreno, S. N. & Docampo, R. A malaria parasite-
638 encoded vacuolar H(+)-ATPase is targeted to the host erythrocyte. *J Biol Chem* **280**,
639 36841-36847 (2005). https://doi.org:10.1074/jbc.M507727200
640 28 Rajaram, K., Liu, H. B. & Prigge, S. T. Redesigned TetR-Aptamer System To Control
641 Gene Expression in Plasmodium falciparum. *mSphere* **5** (2020).
642 https://doi.org:10.1128/mSphere.00457-20
643 29 Ganesan, S. M., Falla, A., Goldfless, S. J., Nasamu, A. S. & Niles, J. C. Synthetic RNA-
644 protein modules integrated with native translation mechanisms to control gene
645 expression in malaria parasites. *Nat Commun* **7**, 10727 (2016).
646 https://doi.org:10.1038/ncomms10727
647 30 Wagner, J. C., Platt, R. J., Goldfless, S. J., Zhang, F. & Niles, J. C. Efficient CRISPR-
648 Cas9-mediated genome editing in Plasmodium falciparum. *Nat Methods* **11**, 915-918
649 (2014). https://doi.org:10.1038/nmeth.3063
650 31 Ghorbal, M. *et al.* Genome editing in the human malaria parasite Plasmodium falciparum
651 using the CRISPR-Cas9 system. *Nat Biotechnol* **32**, 819-821 (2014).
652 https://doi.org:10.1038/nbt.2925
653 32 Ho, C. M. *et al.* Malaria parasite translocon structure and mechanism of effector export.
654 *Nature* **561**, 70-75 (2018). https://doi.org:10.1038/s41586-018-0469-4
655 33 Ressurreicao, M. *et al.* Use of a highly specific kinase inhibitor for rapid, simple and
656 precise synchronization of Plasmodium falciparum and Plasmodium knowlesi asexual
657 blood-stage parasites. *PLoS One* **15**, e0235798 (2020).
658 https://doi.org:10.1371/journal.pone.0235798
659 34 Goldberg, D. E. Hemoglobin degradation in Plasmodium-infected red blood cells. *Semin*
660 *Cell Biol* **4**, 355-361 (1993). https://doi.org:10.1006/scel.1993.1042
661 35 Spielmann, T., Gras, S., Sabitzki, R. & Meissner, M. Endocytosis in Plasmodium and
662 Toxoplasma Parasites. *Trends Parasitol* **36**, 520-532 (2020).
663 https://doi.org:10.1016/j.pt.2020.03.010

36 Jonscher, E. *et al.* PfVPS45 Is Required for Host Cell Cytosol Uptake by Malaria Blood Stage Parasites. *Cell Host Microbe* **25**, 166-173 e165 (2019). https://doi.org:10.1016/j.chom.2018.11.010

37 Milani, K. J., Schneider, T. G. & Taraschi, T. F. Defining the morphology and mechanism of the hemoglobin transport pathway in Plasmodium falciparum-infected erythrocytes. *Eukaryot Cell* **14**, 415-426 (2015). https://doi.org:10.1128/EC.00267-14

38 Wang, R. *et al.* Molecular basis of V-ATPase inhibition by bafilomycin A1. *Nature Communications* **12**, 1782 (2021). https://doi.org:10.1038/s41467-021-22111-5

39 Parra, K. J. & Kane, P. M. Reversible association between the V1 and V0 domains of yeast vacuolar H+-ATPase is an unconventional glucose-induced effect. *Mol Cell Biol* **18**, 7064-7074 (1998). https://doi.org:10.1128/MCB.18.12.7064

40 Parra, K. J., Keenan, K. L. & Kane, P. M. The H subunit (Vma13p) of the yeast V-ATPase inhibits the ATPase activity of cytosolic V1 complexes. *J Biol Chem* **275**, 21761-21767 (2000). https://doi.org:10.1074/jbc.M002305200

41 Stasic, A. J. *et al.* The Toxoplasma Vacuolar H(+)-ATPase Regulates Intracellular pH and Impacts the Maturation of Essential Secretory Proteins. *Cell Rep* **27**, 2132-2146 e2137 (2019). https://doi.org:10.1016/j.celrep.2019.04.038

42 Francis, S. E., Sullivan, D. J., Jr. & Goldberg, D. E. Hemoglobin metabolism in the malaria parasite Plasmodium falciparum. *Annu Rev Microbiol* **51**, 97-123 (1997). https://doi.org:10.1146/annurev.micro.51.1.97

43 Liu, J., Istvan, E. S., Gluzman, I. Y., Gross, J. & Goldberg, D. E. Plasmodium falciparum ensures its amino acid supply with multiple acquisition pathways and redundant proteolytic enzyme systems. *Proc Natl Acad Sci U S A* **103**, 8840-8845 (2006). https://doi.org:10.1073/pnas.0601876103

44 Ludwig, J. *et al.* Identification and characterization of a novel 9.2-kDa membrane sector-associated protein of vacuolar proton-ATPase from chromaffin granules. *J Biol Chem* **273**, 10939-10947 (1998). https://doi.org:10.1074/jbc.273.18.10939

45 Alder, A. *et al.* The role of Plasmodium V-ATPase in vacuolar physiology and antimalarial drug uptake. *Proc Natl Acad Sci U S A* **120**, e2306420120 (2023). https://doi.org:10.1073/pnas.2306420120

46 Meibalan, E. *et al.* Host erythrocyte environment influences the localization of exported protein 2, an essential component of the Plasmodium translocon. *Eukaryot Cell* **14**, 371-384 (2015). https://doi.org:10.1128/EC.00228-14

47 Ling, L. *et al.* Genetic ablation of the mitoribosome in the malaria parasite Plasmodium falciparum sensitizes it to antimalarials that target mitochondrial functions. *J Biol Chem* **295**, 7235-7248 (2020). https://doi.org:10.1074/jbc.RA120.012646

48 Ke, H., Dass, S., Morrisey, J. M., Mather, M. W. & Vaidya, A. B. The mitochondrial ribosomal protein L13 is critical for the structural and functional integrity of the mitochondrion in Plasmodium falciparum. *J Biol Chem* **293**, 8128-8137 (2018). https://doi.org:10.1074/jbc.RA118.002552

A

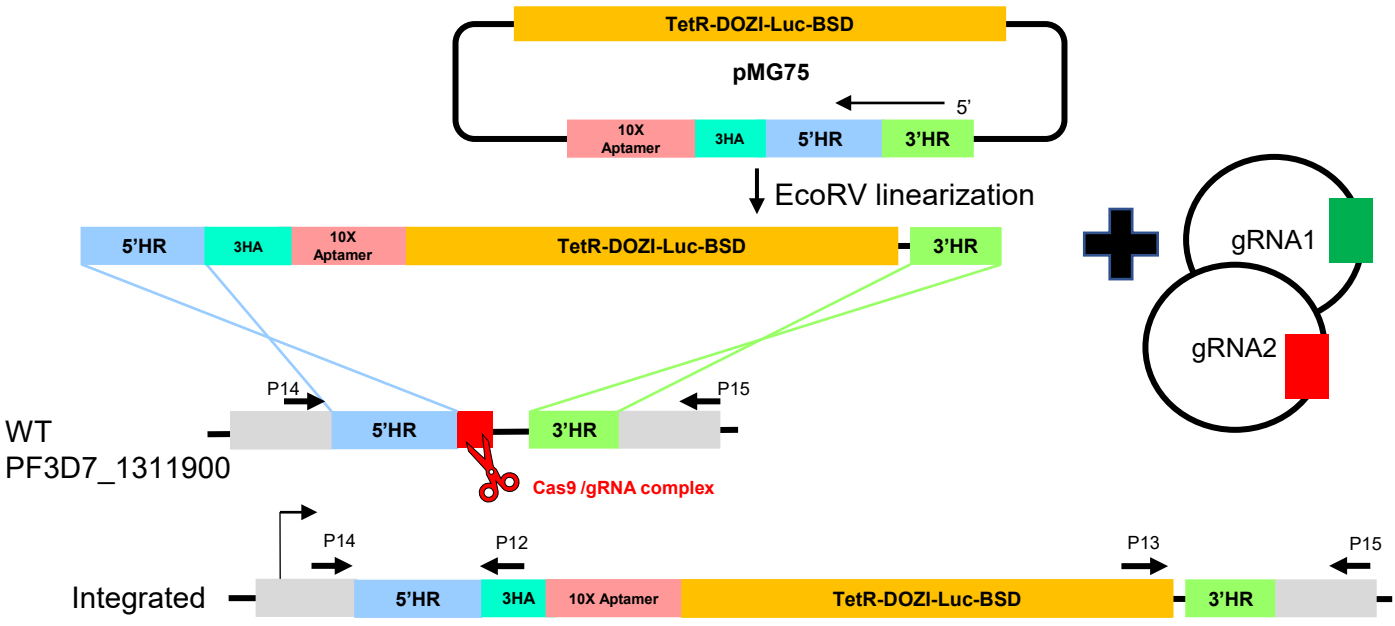


B

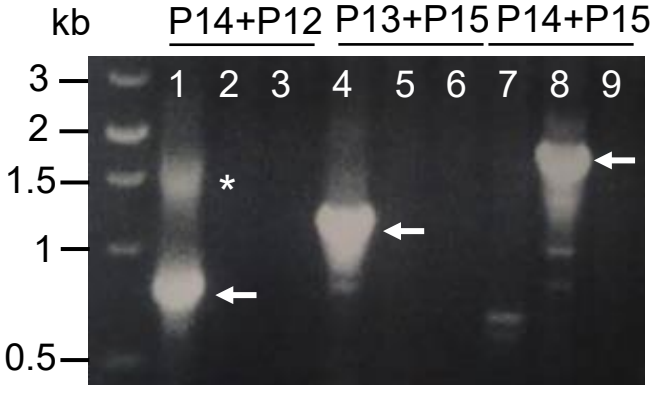


Lanes 1, 4, 7: $V_1A$ transgenic DNA
Lanes 2, 5, 8: WT DNA
Lanes 3, 6, 9: No DNA controls

C

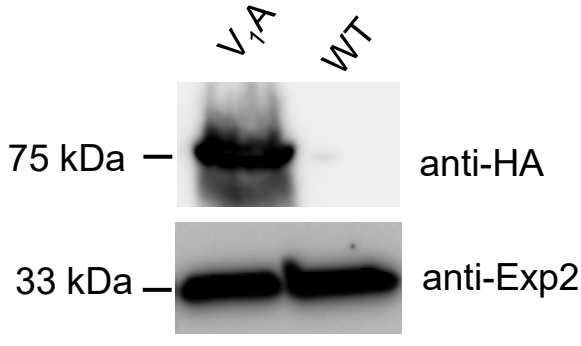


Figure 1. Endogenous tagging of $V_1A$ via CRISPR/Cas9 for conditional expression

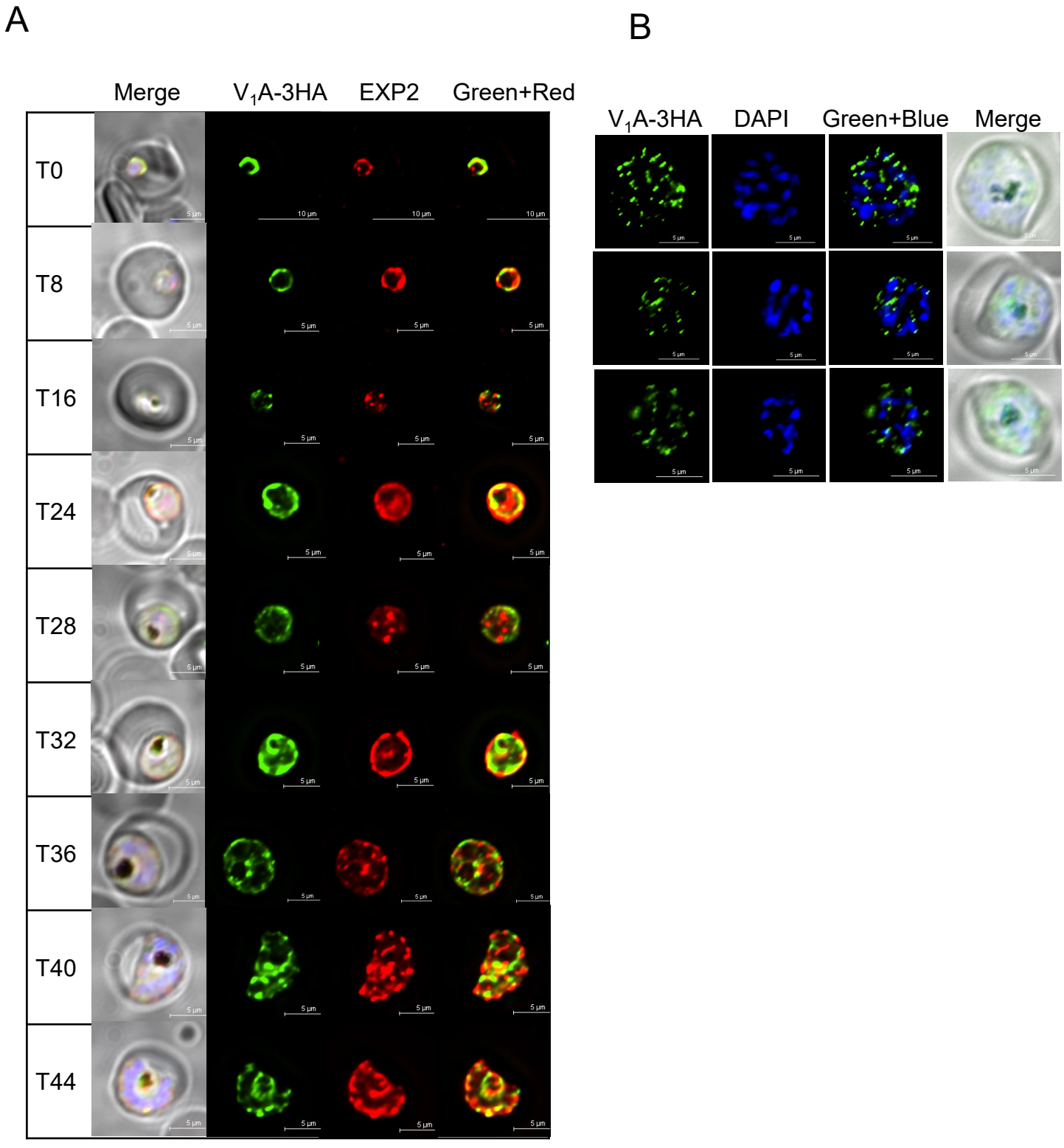


Figure 2. Localization of $V_1A$ throughout the asexual blood stages

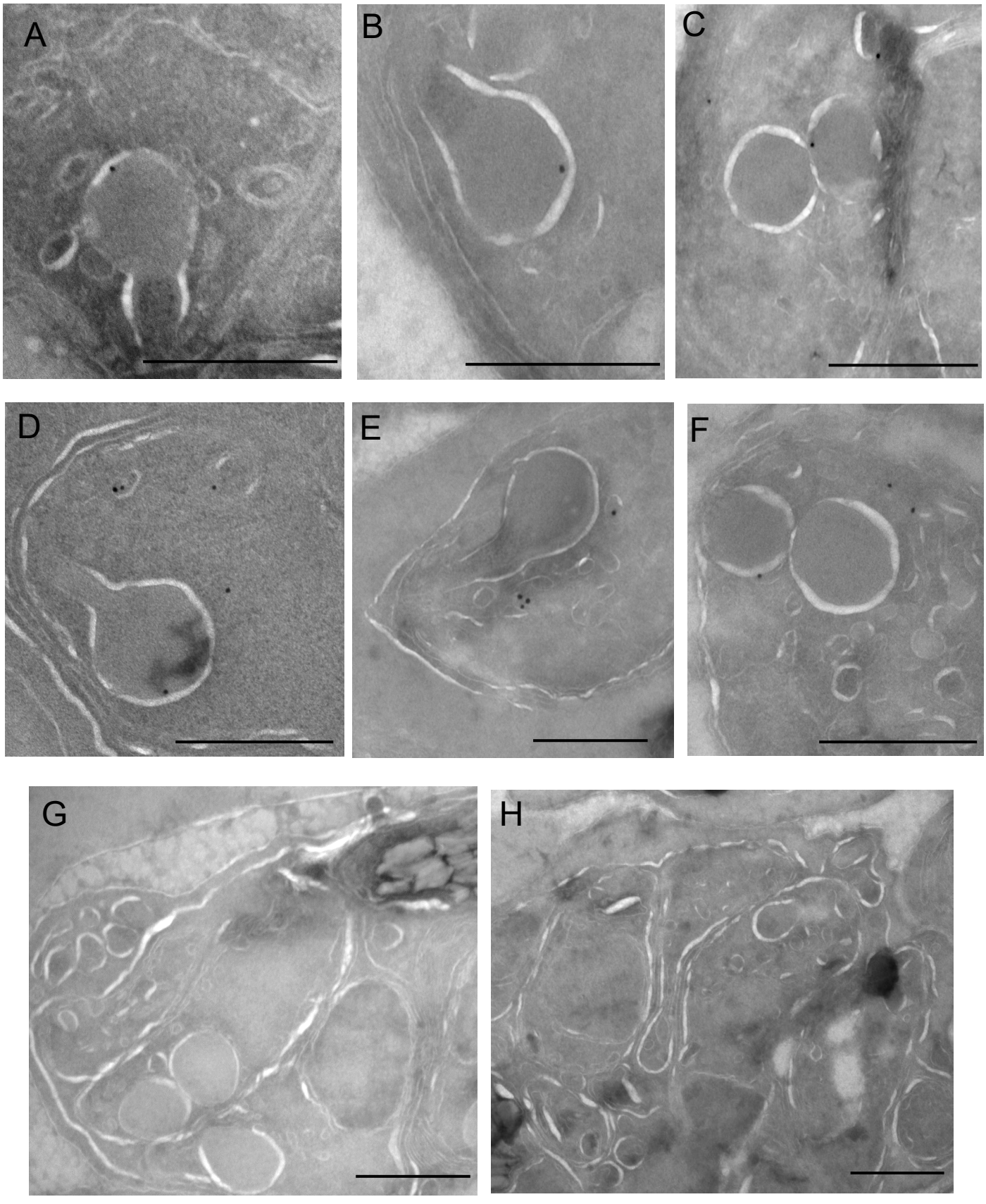


Figure 3. Localization of $V_1A$ on the secretory organelles in mature schizont stage parasites

A

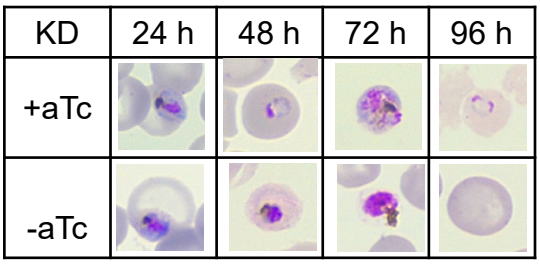


B

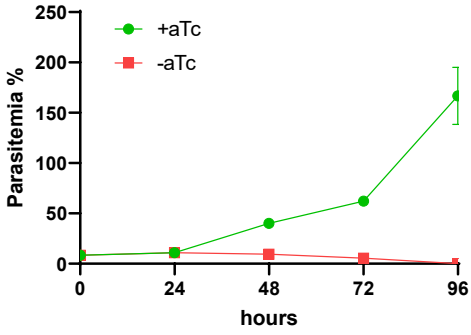


C

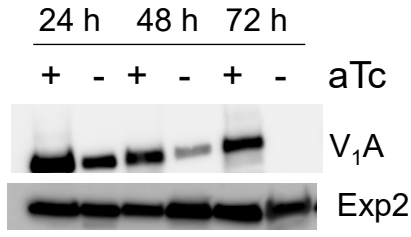


D

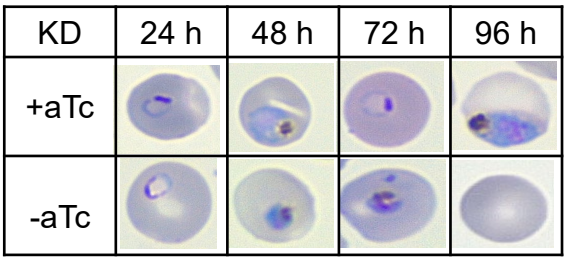


E

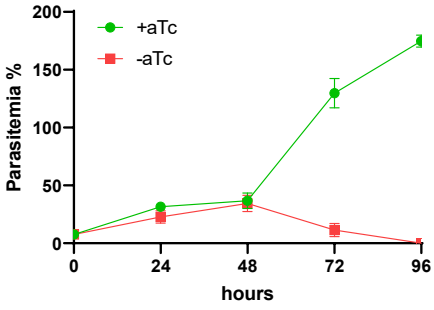


F

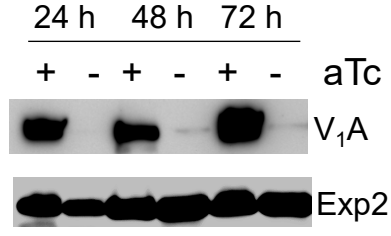


G

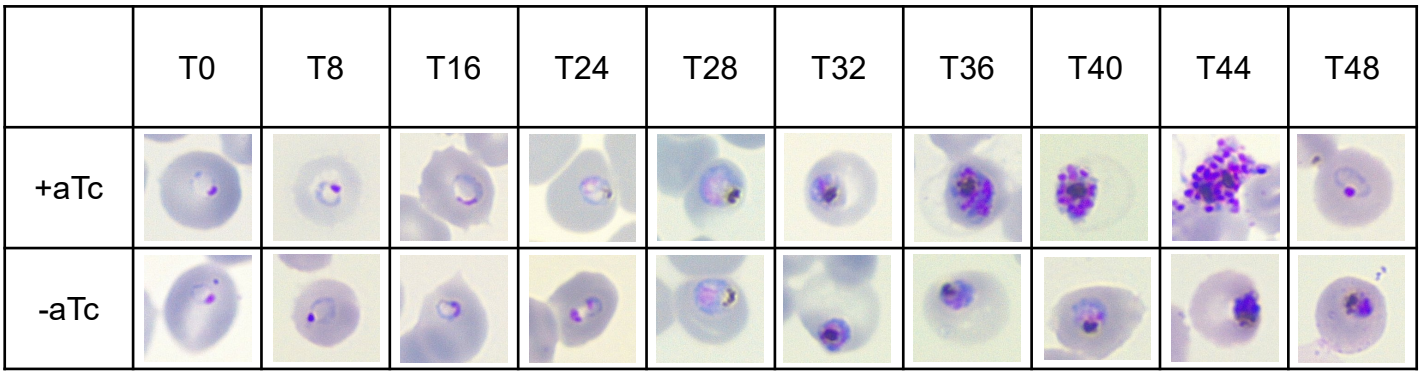


Figure 4. Essentiality of V-type ATPase in the asexual blood stages

A

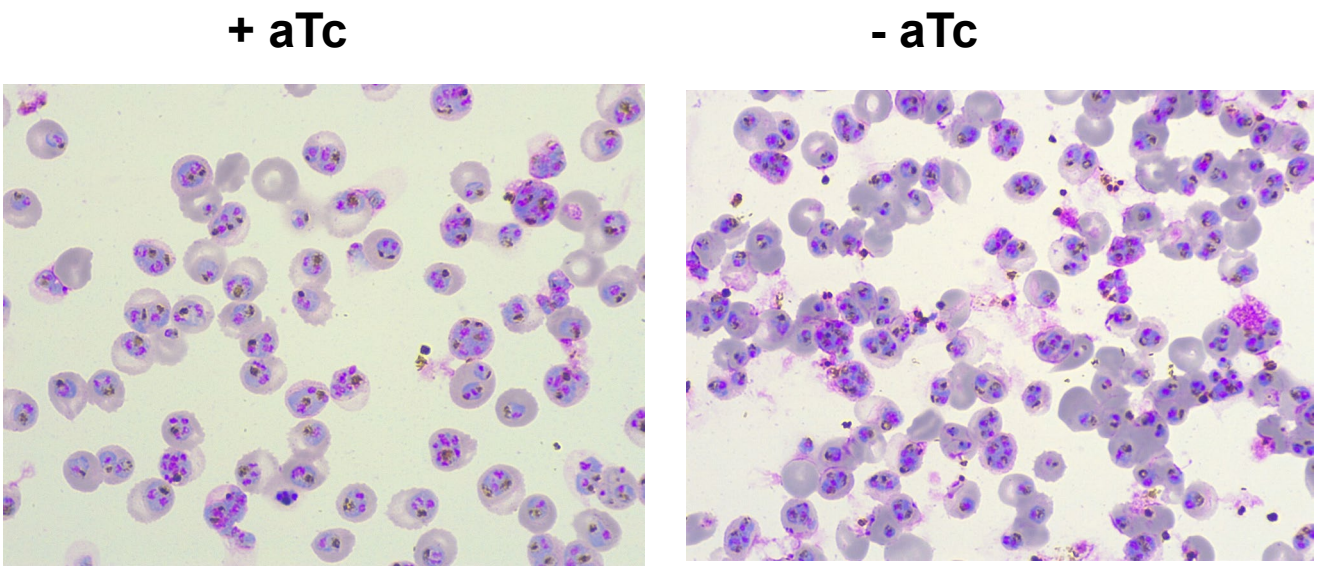


B

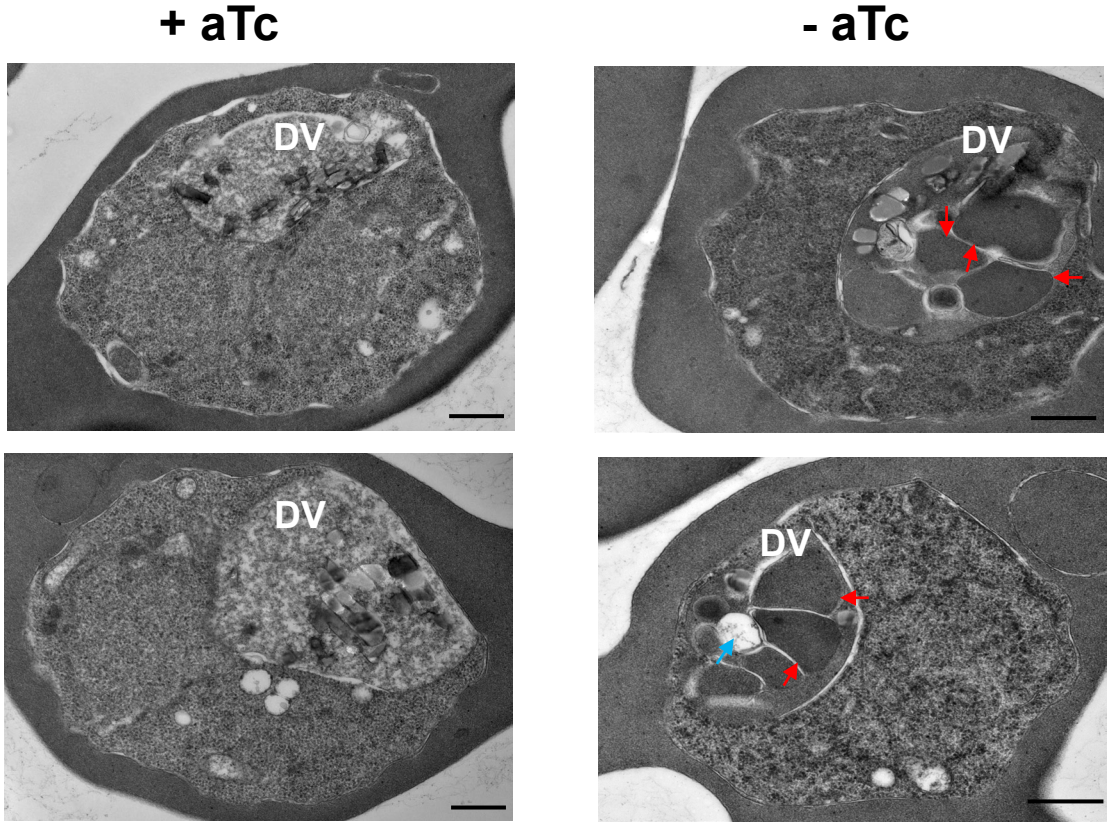


Figure 5. V-type ATPase is essential for hemoglobin digestion in the digestive vacuole

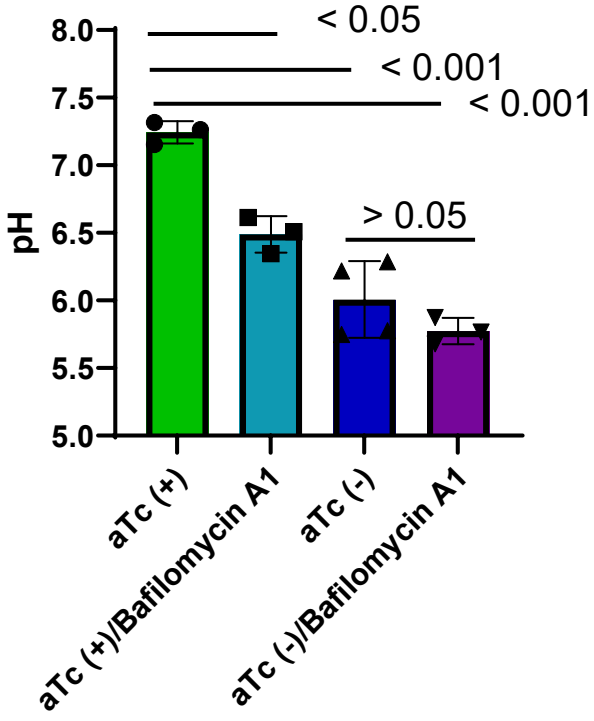


Figure 6. V-type ATPase regulates cytosolic pH in trophozoite stage parasites

A

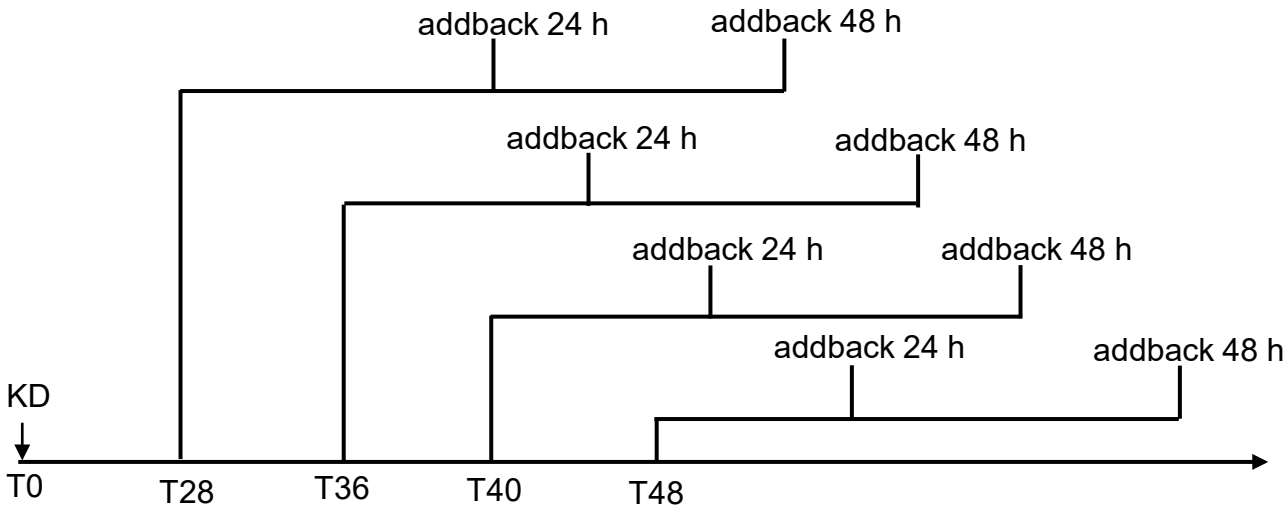


B

| | +aTc | -aTc | addback 24 h | addback 48 h |
|---|---|---|---|---|
| KD 28 h | | | | |
| KD 36 h | | | | |
| KD 40 h | | | | |
| KD 48 h | | | | |

Figure 7. Viability of the V-type ATPase knockdown parasites

A

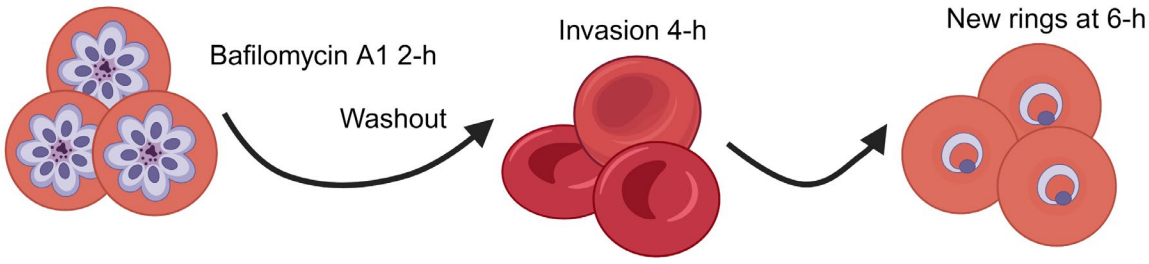


B

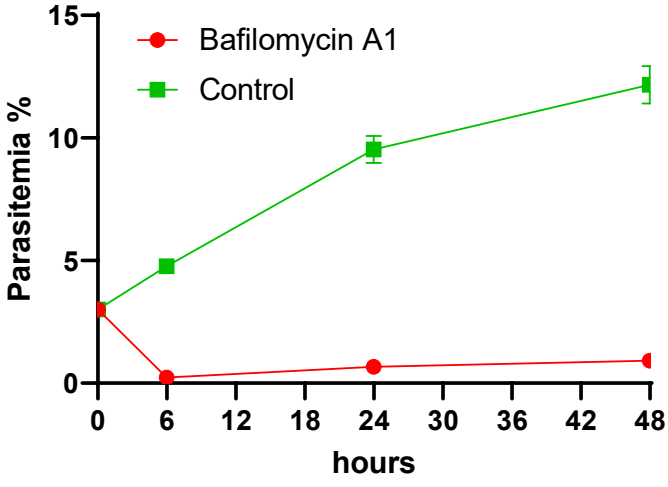


C

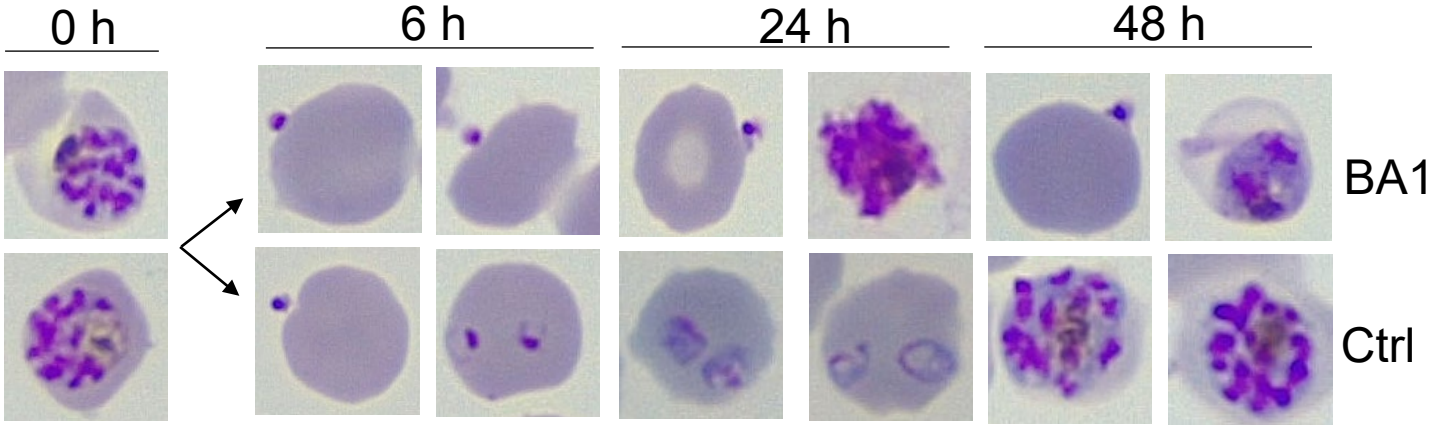


Figure 8. Effects of Bafilomycin A1 on parasite egress and invasion

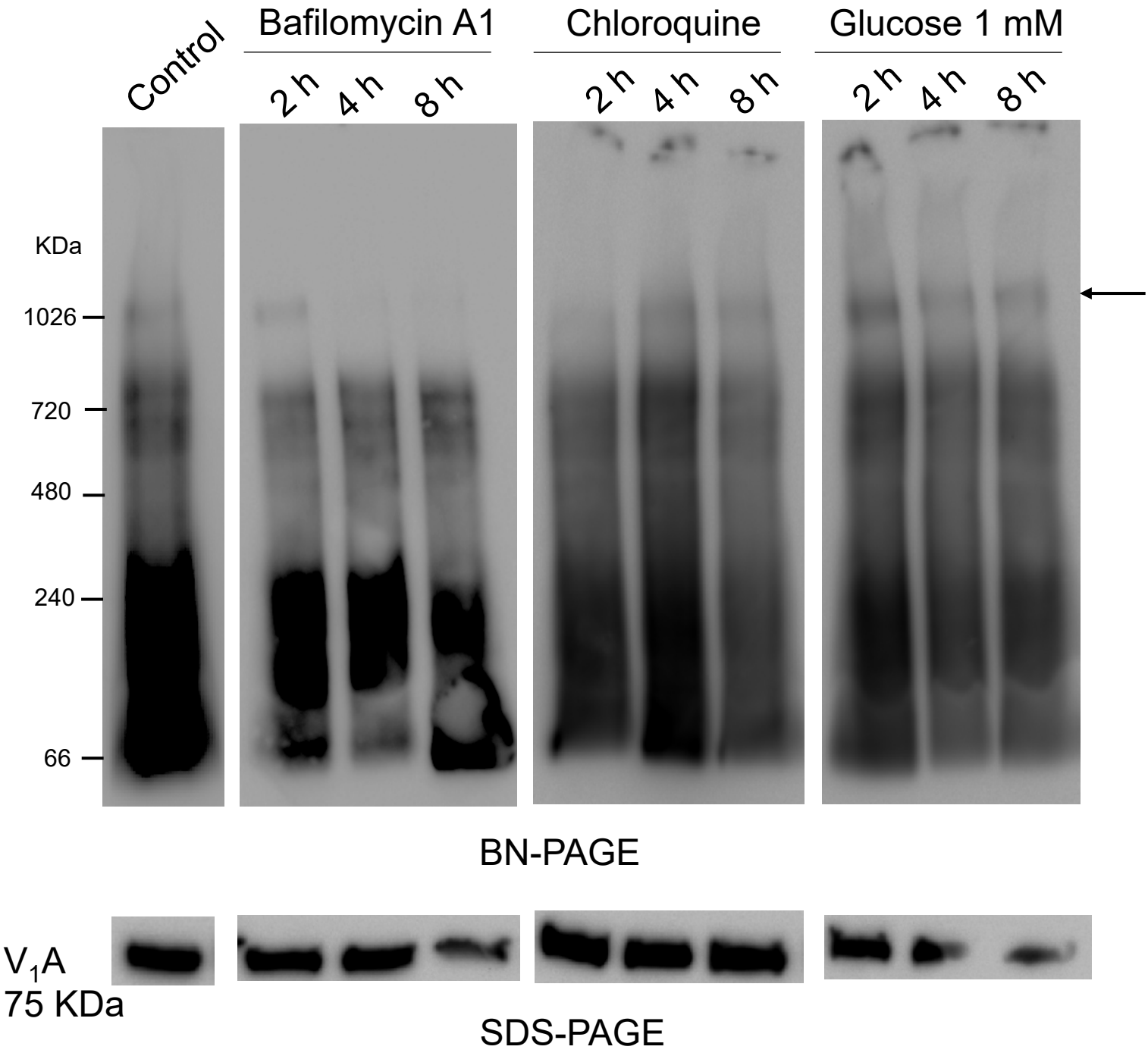


Figure 9. The stability of V-type ATPase complex under various conditions